Bimodal serotonin synthesis in the diurnal rodent, Arvicanthis ansorgei

Rosanna Caputo, Vincent-joseph Poirel, Etienne Challet, Johanna Meijer, Sylvie Raison

RESEARCH ARTICLE

Bimodal serotonin synthesis in the diurnal rodent, *Arvicanthis ansorgei*

Rosanna Caputo[1,2] | Vincent-Joseph Poirel[1] | Etienne Challet[1] | Johanna H. Meijer[2] | Sylvie Raison[1]

[1]Institute of Cellular and Integrative Neurosciences, CNRS and University of Strasbourg, Strasbourg, France

[2]Department of Molecular Cell Biology, Division of Neurophysiology, Leiden University Medical Center, Leiden, the Netherlands

Correspondence
Sylvie Raison, Institute of Cellular and Integrative Neurosciences, CNRS and University of Strasbourg, INCI 8, allée du général Rouvillois, FR 67000 Strasbourg, France.
Email: raison@unistra.fr

Abstract

In mammals, behavioral activity is regulated both by the circadian system, orchestrated by the suprachiasmatic nucleus (SCN), and by arousal structures, including the serotonergic system. While the SCN is active at the same astronomical time in diurnal and nocturnal species, little data are available concerning the serotonergic (5HT) system in diurnal mammals. In this study, we investigated the functioning of the 5HT system, which is involved both in regulating the sleep/wake cycle and in synchronizing the SCN, in a diurnal rodent, *Arvicanthis ansorgei*. Using in situ hybridization, we characterized the anatomical extension of the raphe nuclei and we investigated 24 h mRNA levels of the serotonin rate-limiting enzyme, tryptophan hydroxylase 2 (*tph2*). Under both 12 h:12 h light/dark (LD) and constant darkness (DD) conditions, *tph2* mRNA expression varies significantly over 24 h, displaying a bimodal profile with higher values around the (projected) light transitions. Furthermore, we considered several SCN outputs, namely melatonin, corticosterone, and locomotor activity. In both LD and DD, melatonin profiles display peak levels during the biological night. Corticosterone plasma levels show a bimodal rhythmic profile in both conditions, with higher levels preceding the two peaks of *Arvicanthis* locomotor activity, occurring at dawn and dusk. These data demonstrate that serotonin synthesis in *Arvicanthis* is rhythmic and reflects its bimodal behavioral phenotype, but differs from what has been previously described in nocturnal species.

KEYWORDS

5HT, *Arvicanthis*, circadian, raphe nuclei, rhythm, rodent, SCN, tryptophan hydroxylase 2

Abbreviations: 5HIAA, 5-hydroxyindoleacetic acid; 5HT, serotonin; ACN, acetonitrile; CT, circadian time; DD, constant darkness; DM, dorsomedial subregion of dorsal raphe nucleus; DRN, dorsal raphe nucleus; EDTA, ethylene-diamine-tetra-acetic acid; HPLC, high-pressure liquid chromatography; IGL, intergeniculate leaflet; Lat, lateral subregion of dorsal raphe nucleus; LC, locus coeruleus; LC-MS/MS, liquid chromatography tandem mass spectrometry; LD, light/dark cycle; MRM, multiple reaction monitoring; MRN, median raphe nucleus; OC, optic chiasm; OD, optical density; PBS, phosphate-buffered saline; RCF, relative centrifugal force; RIA, radioimmunoassay; RN, raphe nuclei; RT, room temperature; SCN, suprachiasmatic nucleus; SSC, sodium saline citrate; Tph2, tryptophan hydroxylase 2; VM, ventromedial subregion of dorsal raphe nucleus; VP, vasopressin; ZT, Zeitgeber time.

1 | INTRODUCTION

In mammals, many behavioral and physiological functions are regulated by the circadian system. Circadian rhythms are orchestrated by the master clock, located in the suprachiasmatic nucleus (SCN). The SCN receives timing information from several cues and entrains the rhythmic pattern of various body's physiological and behavioral functions (e.g., fasting/feeding cycle, sleep/wake cycle), by sending neural projections and humoral signals (e.g., melatonin, corticosterone).[1,2] The most potent time cue for the SCN is the light.[3] While a correct functioning of the circadian system is crucial for maintaining optimal health,[4] disruption of circadian rhythms, for example through improper or insufficient exposure to sunlight, may increase the predisposition to develop pathological conditions, including major depressive disorder and seasonal affective disorder.[5-8] Numerous daily rhythms, such as the sleep/wake cycle, hormonal and neurotransmitters' daily oscillations are clearly disrupted in depression.[9] Although the mechanisms underlying the impact of circadian disruption on mood are still unclear, evidence suggests that among the neurotransmitters involved in depression, serotonin (5HT) may play a crucial role.[10,11] Indeed, serotonin occupies a central place in the pathophysiology of depression, as evidenced by antidepressants inhibiting 5HT reuptake, such as citalopram or fluoxetine.[12-14]

Moreover, tight relationships link the 5HT system, the circadian system and many rhythmic physiological functions. Serotonin regulates the sleep/wake cycle by inducing and maintaining wakefulness.[15] Besides, the 5HT system is also involved in the modulation of mood and locomotor activity.[16-18] Furthermore, 5HT plays a role in synchronizing the circadian system, since it is able to shift the phase of the SCN and modulate its synchronization to light.[19-23] In turn, the circadian system exerts its action on many nuclei in the brain, including the serotonergic raphe nuclei (RN). Indeed, both serotonin synthesis and release in the SCN display 24 h variations.[24-29] Evidence in nocturnal rodents suggests that, among the SCN outputs, rhythmic information may be conveyed to the 5HT system via glucocorticoids and locomotor activity.[30,31]

Indeed, behavioral activity correlates with serotonin levels both in nocturnal and diurnal species.[23,32] However, the distribution of rest/activity episodes in nocturnal and diurnal animals occurs at opposite phases relative to the light/dark cycle,[33,34] while the SCN is always active at the same astronomical time.[35-37] Moreover, recent evidence suggests that the effect of serotonin on the circadian system may be different between diurnal and nocturnal species.[23,38] Serotonin antagonizes the effect of light in nocturnal animals, while it strengthens light effect in diurnal species.[39,40]

The current knowledge about the functioning of the serotonergic system and its involvement in mood disorders stems principally from nocturnal models, while little is known about the serotonergic system in diurnal mammals. Considering the differential effects of serotonin in diurnal and nocturnal animals, it is crucial to investigate the functioning of the serotonergic system in a diurnal animal in order to guide studies in humans.

In this study, to gain more insights into the 5HT system in diurnal mammals we used a diurnal rodent, the *Arvicanthis ansorgei*. This species displays a diurnal behavioral phenotype with a crepuscular (or bimodal) pattern of general locomotor activity, with activity peaks at the light/dark and dark/light transitions. We characterized the anatomical extension of the RN and we evaluated serotonin synthesis by quantifying tryptophan hydroxylase 2 (*tph2*) mRNA levels in RN under 12 h:12 h light-dark (LD) cycle and in constant darkness (DD). Furthermore, we have measured SCN contents of serotonin and its main metabolite, 5-hydroxyindoleacetic acid (5HIAA), and we have analyzed several SCN rhythmic outputs as potential modulators of *tph2* expression profile.

This study may help understanding mechanisms that contribute to the phase-inverted outputs of the circadian system between nocturnal and diurnal mammals, so that this knowledge may be more properly translated to humans.

2 | MATERIALS AND METHODS

2.1 | Animals and housing conditions

All experiments were performed in accordance with the guidelines of the European Committee Council Directive of November 24, 1986 (86/609/EEC) and the French Ministry of Higher Education and Research. Adult (5.5 to 10 months of age) male Sudanian grass rats (*A. ansorgei*), weighting 150–250 g, were obtained from our breeding colony (Chronobiotron, UMS 3415, CNRS Strasbourg, France). All the animals were individually housed in Plexiglas cages, raised in 12 h:12 h light/dark (12:12 LD) cycle (light: 150–200 lux, dark: red dim light, <5 lux), and provided with food and water ad libitum. The general locomotor activity of 17 grass rats was recorded every 5 min by a computer-based acquisition system (Circadian Activity Monitoring System; INSERM, Lyon, France) during 4 consecutive days and actograms were analyzed using Clocklab software (Actimetrics, Wilmette, IL, USA).

2.2 | Experimental protocol and samples collection

A total of 84 *Arvicanthis* were entrained to 12:12 LD cycle. Two days before the sacrifice, 42 *Arvicanthis* were exposed to constant darkness (DD), while 42 were maintained in LD. In both conditions, animals were killed by decapitation, after CO_2 sedation, every 4 h (seven time points) starting at *Zeitgeber* time (ZT) 2 for the LD group and at circadian time (CT) 2, for the DD group. The last time point is at ZT2 in LD and CT2 in DD of the second experimental day, indicated as ZT2′ and CT2′, respectively. ZT12 and CT12 were defined as the beginning of dark phase under LD and subjective night in DD, respectively. Trunk blood was collected in hemolysis tubes containing 30 μl of 4% EDTA. Brains were quickly removed and frozen in cold isopentane ($-30°C$) for 1 min 20 s. Plasma samples, resulting from blood centrifugation (15 min, 4000 *g*, 4°C) were stored at $-20°C$, while brains were stored at $-80°C$. Serial coronal 20 μm sections were cut along the caudo-rostral extension of the RN with a cryostat (Leica Instruments GmbH, Nussloch, Germany) and collected on sterile slides. The distance between two collected sections was 100 μm. Since no atlas is available for the *Arvicanthis*, the rat atlas was used as reference (Interaural from +1.9 mm to -0.7 mm, Paxinos & Watson[41]) to morphologically identify the DRN and the MRN. Slides were stored at $-20°C$ until use. For 5HT and 5HIAA quantification, 12 *Arvicanthis* were kept in a 12:12 LD cycle and sacrificed at ZT2, ZT10 and ZT18, while 12 *Arvicanthis* were exposed for 48 h to DD before being sacrificed at CT2, CT10 and CT18 (four animals per group). Brains were quickly removed and frozen in cold isopentane, and subsequently stored at $-80°C$. SCN tissue was microdissected from four consecutive coronal sections (300 μm thickness, 2 mm diameter), using the optic chiasm (OC) as landmark. SCN tissue was stored at $-80°C$ until tissue homogenization.

2.3 | Radioactive in situ hybridization

The sequences for sense and antisense riboprobes were designed based on the rat *tph2* mRNA sequence and were obtained as described by Malek et al.[26] The *tph2* sequence identity was analyzed on the *Arvicanthis niloticus* (taxid:61156) genome using Nucleotide BLAST (https://blast-ncbi-nlm-nih-gov.scd-rproxy.u-strasbg.fr/Blast.cgi), since *A. ansorgei* genome sequence is not available. Probes (495 bp) were transcribed from the corresponding linearized plasmids using the appropriate polymerase (MAXI script; Ambion, Austin, TX) in the presence of [^{35}S]UTP (46.25 GBq/mol, PerkinElmer, Waltham MA). Hybridization with riboprobes on *Arvicanthis* brain slices was performed as follows. Sections were postfixed in 4% formaldehyde for 15 min, rinsed for 2 min in 0.1 M phosphate buffer saline (PBS), acetylated twice for 5 min in 0.4% acetic anhydride in 0.1 M triethanolamine (pH 8.0), rinsed for 2 min in 0.1 M PBS, dehydrated in graded ethanol series, and air dried. Hybridization was carried out by depositing 80 μl of riboprobes (400 pm) in a solution containing 50% deionized formamide, 2X sodium saline citrate (SSC), 1X Denhardt's solution, 0.25 mg/ml yeast totalRNA, 1 mg/ml salmon sperm DNA, 10% dextran sulfate, and 400 mM dithiothreitol. Sections were placed in humid boxes containing 2X SSC/50% formamide at 54°C overnight. After hybridization, the sections were washed for 5 min in 2X SSC and then treated with ribonuclease A (10 μg/μl; Sigma St. Quentin Fallavier, France) for 30 min at 37°C. Stringency washes were performed in 1X SSC for 5 min at room temperature (RT) and then in 0.05X SSC for 30 min at 52°C. Sections were finally dehydrated in graded ethanol series, air dried at RT and then exposed to an autoradiographic film (Kodak BioMax; Kodak, Rochester, NY), with a ^{14}C standard.

2.4 | HPLC measurement of 5HT and 5HIAA SCN levels

SCN punches were homogenized by sonication in 0.1 mM Ascorbic Acid and centrifuged at 20.000 RCF. Twenty pmol of D4-serotonin and 30 pmol of D5-hydroxyindoleacetic acid (5HIAA) internal standards were added to all samples before sample treatment. Four volumes of ice-cold acetonitrile (ACN) were added to all samples, which were then centrifuged at 20.000 RCF for 20 min at 4°C. The resulting supernatants were placed in the speed vacuum until samples were completely dry. Samples were then suspended in 0.1 M formic acid, centrifuged at 20.000 RCF for 20 min at 4°C, and the upper phase was recovered to perform LC-MS/MS analyses. Only for serotonin and D4-serotonin, the AccQTag derivation protocol was performed before adding ACN. Analyses were performed on a Dionex Ultimate 3000 High-Pressure Liquid Chromatography (HPLC) system (Thermo Scientific) coupled with a triple-quadrupole Endura (Thermo Scientific). The system was controlled by Xcalibur Software version 2.0 (Thermo Electron, Villebon Sur Yvette, France). Five μl of each sample was loaded into an Accucore RP-MS column (reference P.N. 8636600-902, Zorbax SB/C18 micro bore rapid resolution 1.0 × 150 mm 3.5 μm, Agilent) heated at 40°C. All molecules and the deuterated compounds were eluted by applying a gradient of buffer A and buffer B. Buffer A was 1% acetonitrile (ACN)/98.9% H_2O/0.1% formic acid (v/v/v), whereas buffer B was 99.9% ACN/0.1% formic acid (v/v). The following multi-step

gradient was applied: a linear gradient of 0%–20% of solvent B at 0.09 ml/min during 6.5 min, followed by a linear gradient of 20%–98% of solvent B for 2 min, 1 min at 95% of solvent B and a linear gradient of 0.5 min of 98%–0% of buffer B. Qualitative analysis and quantification was performed in the multiple reaction monitoring (MRM) mode, using Quan Browser software (Thermo Scientific). For ionization, 3500 V of liquid junction voltage and 297°C capillary temperature was applied. The selectivity for both Q1 and Q3 was set to 0.4 Da (FWHM). The collision gas pressure of Q2 was set at 2 mTorr of argon. For all molecules, the selection of the monitored transitions and the optimization of the collision energy (CE) were first determined. The transitions and the corresponding CEs used for MRM mode were the following: 347.13 charge/mass ratio (m/z) → m/z 171 (CE = 27.55 eV) for 5-HT; m/z 351.16 → m/z 171 (CE = 28.1 eV) for D4-serotonin; m/z 192.12 → m/z 118.11 (CE = 28.65 eV), m/z 91.17 (CE = 34.88 eV), and m/z 146.06 (CE = 14.55 eV) for 5-HIAA; and m/z 197.14 → m/z 122.11 (CE = 29.1 eV), m/z 150.04 (CE = 15.61 eV), and m/z 151.07 (CE = 15.91 eV) for D5–5-HIAA. Identification was based on precursor ions, daughter ions and retention times. Quantification was performed calculating the ratio of daughter ions response areas of the internal standards. Data were normalized to grams of proteins.

2.5 | HPLC measurement of corticosterone plasma levels

For corticosterone quantification, *Arvicanthis* samples were processed as follows. Fifty pmol of D4-corticosterone were added to 50 μl of each plasma sample. After adding 1 ml of ice-cold acetonitrile (ACN), samples were incubated at 4°C for 70 min and then centrifuged at 20.000 RCF for 20 min at 4°C. The upper phase was recovered, and a step of centrifugation was repeated in the same conditions. The resulting supernatants were placed in the speed vacuum until samples were completely dry. Samples were subsequently suspended in 20% ACN/0.1% formic acid (v/v), before to perform LC-MS/MS analyses. Analyses were performed on a Dionex Ultimate 3000 High-Pressure Liquid Chromatography system (Thermo Scientific) coupled with a triple-quadruple Endura (Thermo Scientific). The system was controlled by Xcalibur Software version 2.0 (Thermo Scientific). Samples were loaded into an Accucore RP-MS column (reference P.N. 8636600-902, Zorbax SB/C18 micro bore rapid resolution 1.0 × 150 mm 3.5 μm, Agilent) heated at 40°C. Corticosterone and its deuterated compound were eluted by applying a gradient of buffer A and buffer B. Buffer A was 1% ACN/98.9% H_2O/0.1% formic acid (v/v/v), whereas buffer B was 99.9%

ACN/0.1% formic acid (v/v). The following multi-step gradient was applied: a linear gradient of 0%–25% of solvent B at 0.09 ml/min during 2 min, followed by a linear gradient of 25%–30% of solvent B for 7 min, a linear gradient of 30%–98% of solvent B for 2 min, 2 min at 95% of solvent B and a linear gradient of 1 min of 98%–0% of buffer B. Qualitative analysis and quantification was performed in the MRM mode, using Quan Browser software (Thermo Scientific). For ionization, 3500 V of liquid junction voltage and 297°C capillary temperature was applied. The selectivity for both Q1 and Q3 was set to 0.7 Da (FWHM). The collision gas pressure of Q2 was set at 2 mTorr of argon. For all molecules, the selection of the monitored transitions and the optimization of the collision energy (CE) were first determined. The transitions and the corresponding CEs used for MRM mode were the following: m/z 347.11 → m/z 293.47 (CE = 17.03 eV), m/z 311.29 (CE = 15.92 eV), and m/z 329.17 (CE = 14.95 eV) for Corticosterone; and m/z 351.18 → m/z 297.10 (CE = 17.69 eV), m/z 315.18 (CE = 16.88 eV), and m/z 333.24 (CE = 15.56 eV) for D5–corticosterone. Identification was based on precursor ions, daughter ions and retention times. Quantification was performed by calculating the ratio of daughter ions response areas of the internal standards. Data were normalized to milliliters of plasma.

2.6 | Radioimmunoassay of melatonin plasma levels

Melatonin plasma concentrations were measured using a melatonin radioimmunoassay (RIA) kit (Bühlmann Laboratories AG, Schönenbuch, Switzerland) by a double-antibody based on the Kennaway G280 anti-melatonin antibody (rabbit polyclonal antibody). Reversed-phase column extracted samples and controls and reconstituted calibrators were incubated with the anti-melatonin antibody and 125I-melatonin. The sensitivity of the method is 0.3 pg/ml, the intra-assay variability less than 7.9% and inter-assay variability 8.2%. Samples were extracted on columns after conditioning with 2 × 1 ml of methanol and 2 × 1 ml of water. Sample was loaded on column and washed twice with 1 ml 10% (v/v) methanol, and 1 ml of hexane. Melatonin was eluted in 1 ml of methanol. Samples were evaporated to dryness and subsequently reconstituted in 1 ml of incubation buffer. Samples were split and run in duplicates. 100 μl of antiserum and 100 μl of tracer were added to samples (400 μl), and incubated 20 h at 4°C. After incubation, 100 μl of second antibody were added and samples were incubated 15 min at 4°C. One ml of deionized water was added and samples were centrifuged at 2000 g for 2 min at 4°C. The supernatant was aspirated, and radioactivity was counted in a Gamma

counter. Five standards were included: A 0.5 pg/ml, B 1.5 pg/ml, C 5.0 pg/ml, D 15.0 pg/ml, E 50.0 pg/ml.

2.7 | Quantitative analyses of *tph2* mRNA

Quantitative analyses of the autoradiograms were performed by using NIH ImageJ software. Specificity of the antisense probe was tested by hybridization of the antisense and sense probes in the *Arvicanthis* and rat raphe, and in the *Arvicanthis* locus coeruleus (LC) as shown in Figure 1. In *Arvicanthis*, *tph2* hybridization allowed accurate identification of the DRN and MRN. Furthermore, subregions of the DRN can be distinguished: ventromedial (VM), dorsomedial (DM) and two lateral (Lat) groups
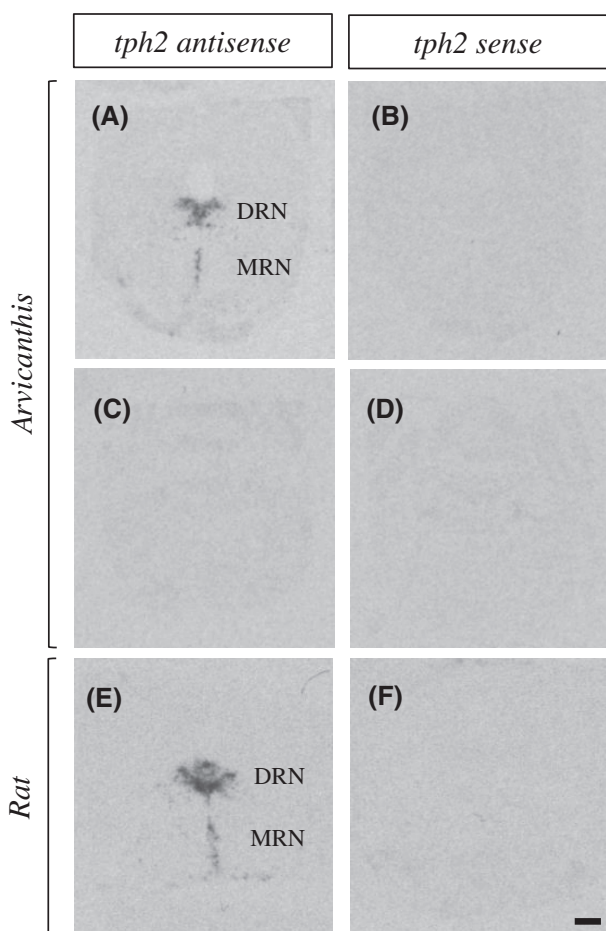

FIGURE 1 Riboprobe quality control. In situ hybridization performed on coronal sections of *Arvicanthis* (A, B, C and D) and rat (E and F) using *tph2* riboprobes antisense (A, C and E) and sense (B, D and F). *Tph2* antisense riboprobe labels the dorsal raphe nucleus (DRN) and the median raphe nucleus (MRN) in *Arvicanthis* (A) and in rat (E). No specific labeling on the *Arvicanthis* locus coeruleus (LC) using *tph2* antisense riboprobe (C) and on the *Arvicanthis* DRN and MRN (B), LC (D), or rat DRN and MRN (F) using *tph2* sense riboprobe. Scale bar: 750 μm

(Figure 2). Six 20 μm coronal sections (distance between two sections = 100 μm) along the caudo-rostral extension of the median part of the DRN and the MRN (Figure 2), were analyzed. For each section, the total optical density (OD) was measured in each subregion of the DRN and in the MRN, and the specific signal intensity was calculated by subtracting the non-specific OD, measured in the mesencephalic surrounding area, where the signal was not specific. OD was normalized to relative levels of mRNA, using a ^{14}C radioactive scale (KBq/g).

2.8 | Statistical analyses

To test the distribution of the mRNA expression across the caudo-rostral extension of the *Arvicanthis* raphe among the seven time points, two-way analysis of variance (ANOVA II) was performed, with factors "time," "section" and their interaction. The effect of light condition (LD vs DD) was tested by the three-way analysis of variance (ANOVA III), with factors "time," "light condition," "section" and the interaction between "time" and "light condition." *Post-hoc* analyses were performed to examine the significant difference among time points and among sections. For HPLC data of 5HT, 5HIAA and 5HT/5HIAA ratio, differences among time points within the same light condition were analyzed using ANOVA I and multiple *t*-tests. Furthermore, differences between light conditions were analyzed using an ANOVA II, with factors "time," "light condition" and their interaction. Melatonin data were analyzed using an ANOVA II, with factors "time," "light condition" and their interaction. *Arvicanthis* corticosterone data were analyzed using an ANOVA II, with factors "time," "light condition" and their interaction. Data were fitted by a non-linear regression using Cosinor analysis (SigmaPlot software, Jandel Scientific, Chicago, IL, USA). These analyses were performed using the following equation: Bimodal (12 h) rhythm: $y = A + (B_* \cos(2\pi(\times - C)/12))$; where A is the mean level (mesor), B the amplitude and, C the acrophase of the rhythm. Locomotor activity was recorded for 17 *Arvicanthis*, in LD over 4 days. For each animal, the average locomotor activity counts over each hour are converted in percentage of total counts. The effect of time on mean hourly data was tested by an ANOVA I and data were fitted by non-linear regression using Cosinor analysis (as previously described). For all statistical procedures, the level of significance was set at $p < .05$. All data are presented as mean ± SEM, unless otherwise stated. The following *Post-hoc* analyses were performed: Dunn's Method for ANOVA I, Bonferroni test for ANOVA II, and Holm-Sidak test for ANOVA III. Sigma Plot (v14) and SPSS (v22) software were used for statistical analyses.
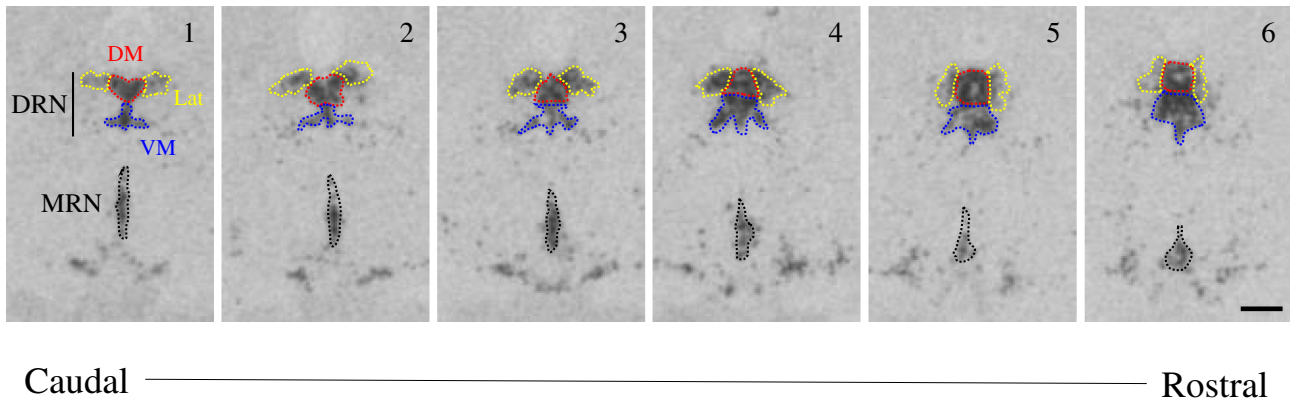
FIGURE 2 In situ hybridization of *tph2* riboprobe of *Arvicanthis* dorsal raphe nucleus (DRN) and median raphe nucleus (MRN, black dotted lines), and identification of DRN subdivisions into lateral (Lat, yellow dotted lines), dorsomedial (DM, red dotted lines) and ventromedial (VM, blue dotted lines) regions. Six successive sections are considered along the caudo-rostral raphe extension. Each section is 20 μm thick and the interval between two sections is 100 μm. Scale bars: 700 μm

3 | RESULTS

3.1 | Technical validation

The sequences for *tph2* riboprobes were designed based on the rat *tph2* mRNA sequence. Since the *A. ansorgei* genome is not available, *tph2* similarity was tested on the *A. niloticus* sequence. BLAST analysis revealed 93.94% identity with *A. niloticus* predicted *tph2* mRNA sequence. In situ hybridization of antisense riboprobe for *tph2* clearly labeled the *Arvicanthis* DRN and MRN (Figure 1A). Specificity of the probe was tested on coronal sections of the *Arvicanthis* locus coeruleus (LC), where no presence of *tph2* is expected. Indeed, no specific signal was detected on LC section (Figure 1C). Rat coronal section of DRN and MRN was used as positive control (Figure 1E). Hybridization of sense *tph2* riboprobe showed no specific signal neither in the *Arvicanthis*/rat DRN or MRN (Figure 1B,D), nor in the *Arvicanthis* LC (Figure 1F). Significant OD variations were measured in the RN, while non-specific OD measured in the mesencephalic surrounding area was constant.

3.2 | Anatomical organization of the *Arvicanthis* raphe nuclei

Raphe nuclei are characterized by different subregions, which in other species have been described as anatomically and functionally independent nuclei. It is still not known whether different raphe subgroups may be identified in *Arvicanthis*. Hybridization with *tph2* antisense riboprobe allowed an anatomical characterization of the *Arvicanthis* DRN and MRN. As shown in Figure 2, three subregions of DRN were delineated: dorsomedial (DM),

ventromedial (VM) and two lateral (LAT) groups. We identified these subgroups in six successive 20 μm sections along the caudo-rostral extension of the DRN. In the same sections, the MRN was identified ventrally to the DRN.

3.3 | *tph2* mRNA profile within the *Arvicanthis* raphe nuclei

Tph2 mRNA expression was quantified in DRN subdivisions and in MRN every 4 h for seven time points, in LD and DD conditions (Figure 3). In LD, a significant effect of time on *tph2* expression is observed in all the three subregions of the DRN (ANOVA II; Lat: $p < .001$, DM: $p = .003$, VM: $p < .001$), and in the MRN (ANOVA II; $p = .049$), as shown in Figure 3A. Overall, *Post-hoc* analyses revealed two higher time points of *tph2* mRNA levels close to the light transitions at ZT10 and at ZT2, while two lower time points are observed at ZT6 and at ZT22. Indeed, significant decreases in *tph2* levels is measured at ZT6 versus ZT2 and versus ZT10 and at ZT22 versus ZT2 and versus ZT10 (Table S1). In DD as well, time had a significant effect on *tph2* mRNA levels in Lat, DM, VM and in MRN (ANOVA II; $p < .001$, $p = .003$, $p < .001$, $p < .001$, respectively), as shown in Figure 3B. Higher *tph2* expression is observed at CT22, while lower expression is measured at CT18, CT6 and CT2′ (Table S1). Cosinor analyses showed a significant bimodal fit of *tph2* mRNA expression in the Lat DRN and MRN under DD conditions (Table S2). The peak values are at CT10.9 and CT22.9 in Lat DRN, and at CT10.8 and CT22.8 in MRN. In addition, a different *tph2* expression profile is observed between the LD and DD conditions. In all the four structures, *Post-hoc* analyses show that
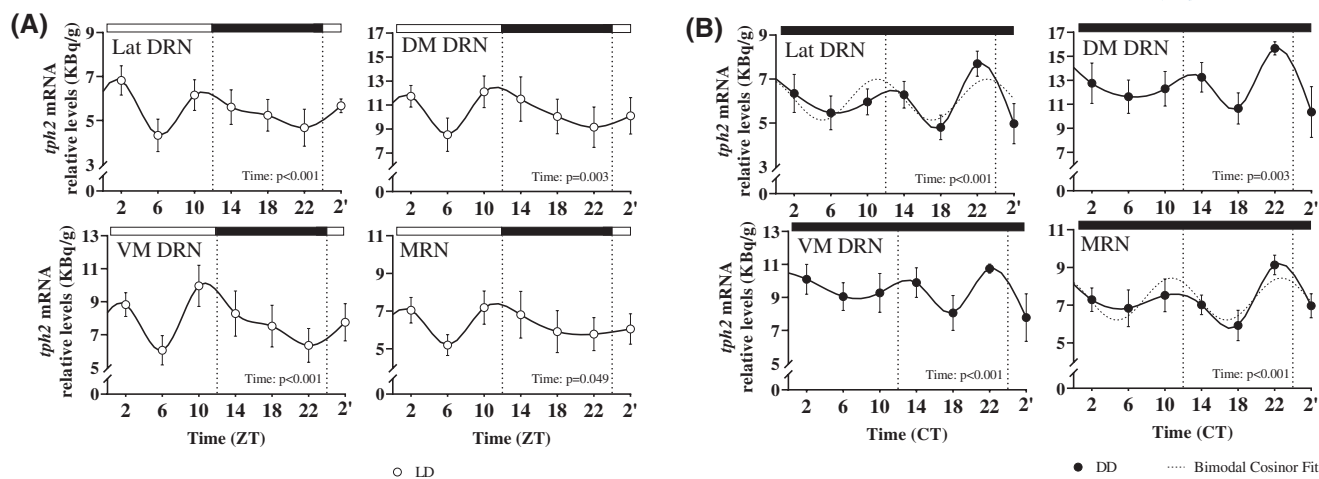
FIGURE 3 In situ hybridization measurements of *tph2* mRNA relative levels within the lateral (Lat), dorsomedial (DM), ventromedial (VM) subregions of the dorsal raphe nucleus (DRN) and in the median raphe nucleus (MRN) in *Arvicanthis* housed in 12 h:12 h light/dark (LD, open circles) (A) and constant darkness (DD, filled circles) (B) conditions. Points are connected by a smoothing line. The effect of time on *tph2* expression is significant in all conditions. Dashed line in Lat DRN and MRN (B) represents the bimodal Cosinor fit. Experimental groups were all $n \geq 5$, except for MRN at CT2′ ($n = 4$). Data are presented as mean ± SEM. Time is expressed as *Zeitgeber* time (ZT) or circadian time (CT). White and black horizontal bars represent light and dark phases, respectively
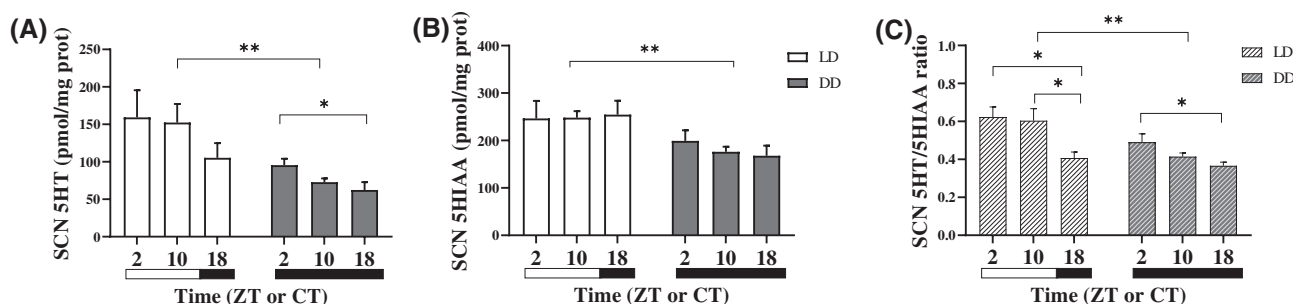
FIGURE 4 Serotonin (5HT, A) and 5-hydroxyindolacetic acid (5HIAA, B) concentration in the SCN of *Arvicanthis* measured by HPLC in LD (white bars) and DD (gray bars). 5HT/5HIAA ratio (C) under LD (white striped bars) and DD (gray striped bars) conditions. Significant effect of time and of light condition is represented with one asterisk (*) when $p < .05$ and by two asterisks (**) when $p < .01$. Data are presented as mean ± SEM. Experimental groups were all $n = 4$, except for CT2 ($n = 5$). Time is expressed as *Zeitgeber* time (ZT) or circadian time (CT). White and black horizontal bars represent light and dark phases, respectively

the differences between the two profiles is significant at the time points ZT6 versus CT6 (Holm-Sidak test; Lat: $p = .045$; DM: $p = .004$; VM: $p < .001$; MRN: $p = .015$), and ZT22 versus CT22 (Holm-Sidak test; Lat: $p < .001$; DM: $p < .001$; VM: $p < .001$; MRN: $p < .001$).

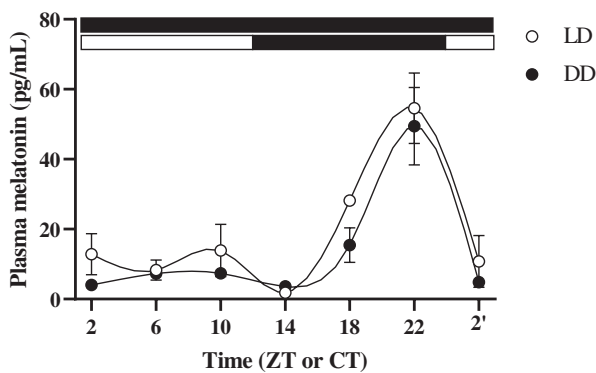## 3.4 | 5HT and 5HIAA levels in the *Arvicanthis* SCN area in LD and DD

Serotonin (5HT) and its main metabolite 5-hydroxyindoleacetic acid (5HIAA) were quantified by HPLC in the SCN of *Arvicanthis* sacrificed at three time points across the LD cycle (ZT2, ZT10, ZT18), and three time points in constant darkness (CT2, CT10, CT18). We observed a significant effect of time on 5HT concentration (ANOVA I; $p = .048$) under DD cycle, with higher levels at CT2 compared to CT18 (*t*-test; $p = .042$) (Figure 4A). In addition, a significant effect of time on 5HT/5HIAA ratio in LD (Figure 4C, ANOVA I; $p = .028$) is observed, with higher ratio at ZT2 and ZT10 compared to ZT18 (*t*-test: $p = .013$ and $p = .033$, respectively). In DD, a significant higher 5HT/5HIAA ratio is measured at CT2 compared to CT18 (*t*-test; $p = .047$). Significant lower concentrations of both 5HT (Figure 4A, ANOVA II; $p = .001$) and 5HIAA (Figure 4B, ANOVA II; $p = .003$), as well as a lower 5HT/5HIAA ratio (Figure 4C, ANOVA II; $p = .003$), were measured in DD compared to LD cycle.

3.5 | Plasma melatonin levels of *Arvicanthis* housed in LD and DD

Melatonin is one of the main outputs of the SCN, and a strong indicator of the circadian phase. Plasma melatonin concentration was measured by radioimmunoassay in LD and DD conditions. In both light conditions, melatonin levels significantly changed over time (Figure 5, ANOVA II; $p < .001$), with low levels during the (subjective) day and a peak at ZT or CT22 ($p < .001$ compared with all the other time points). No significant difference is measured between the LD and DD melatonin profiles (ANOVA II; light condition: $p = .089$, interaction: $p = .989$).

3.6 | Plasma corticosterone levels of *Arvicanthis* housed in LD and DD

As shown in Figure 6A,B, plasma levels of corticosterone significantly varied over time, both in LD (ANOVA I; $p = .017$) and DD (ANOVA I; $p = .004$) conditions. A significant increase at ZT22 was measured in LD compared to ZT18, and at CT22 in DD compared to CT18 and CT14. Cosinor analyses revealed a significant bimodal rhythm over 24 h both in LD ($p < .001$, $R^2 = .312$; Figure 6A), and in DD ($p < .001$, $R^2 = .266$, Figure 6B). The two peaks of corticosterone are observed at ZT10.5 and ZT22.5 in LD, and at CT9.5 and CT21.5 in DD. ANOVA II did not show any significant difference between LD and DD corticosterone profiles (light condition: $p = .633$, interactions: $p = .572$).

3.7 | General locomotor activity of *Arvicanthis* in LD

Locomotor activity data were analyzed for seventeen of the *Arvicanthis* housed in LD condition. All the animals were more active during the day than during the night. Indeed, $71.6\% \pm 1.8\%$ of the activity occurred during the day and $28.9\% \pm 1.8\%$ during the night (ANOVA I; $p < .001$, Figure 7A). Sixteen *Arvicanthis* showed a bimodal pattern of activity, with higher percentage of the activity occurring at the light/dark and dark/light transitions. One *Arvicanthis* had a unimodal locomotor activity profile, with higher activity occurring throughout the light phase (data not shown). Figure 7B shows the mean daily locomotor activity profile, expressed as hourly percentage of counts. The effect of time is significant (ANOVA I; $p < .001$), and data are significantly fitted by a bimodal Cosinor regression ($p < .0001$, $R^2 = .332$; Figure 7B). The two peaks of activity

FIGURE 5 Melatonin plasma levels measured by radioimmunoassay. ANOVA II reveals a significant effect ($p < .001$) of the time in both LD (open circles) and DD (filled circles) conditions. Points are connected by a smoothing line. Data are presented as mean ± SEM. All experimental groups were $n \geq 5$, except for ZT6 ($n = 2$), ZT14 ($n = 3$) ZT18 ($n = 4$) and ZT22 ($n = 3$). Time is expressed as *Zeitgeber* time (ZT) or circadian time (CT). White and black horizontal bars represent light and dark phases, respectively
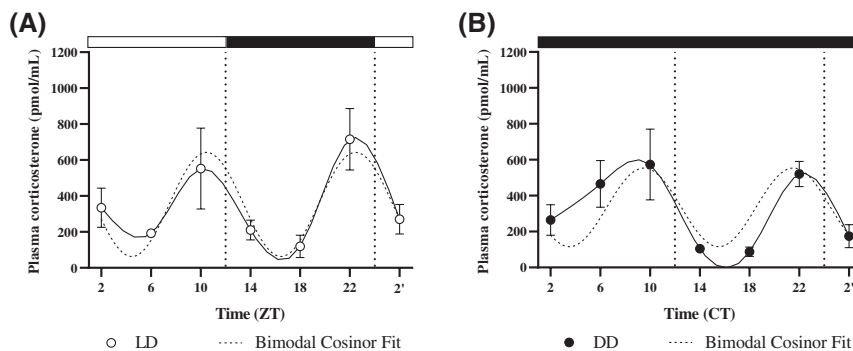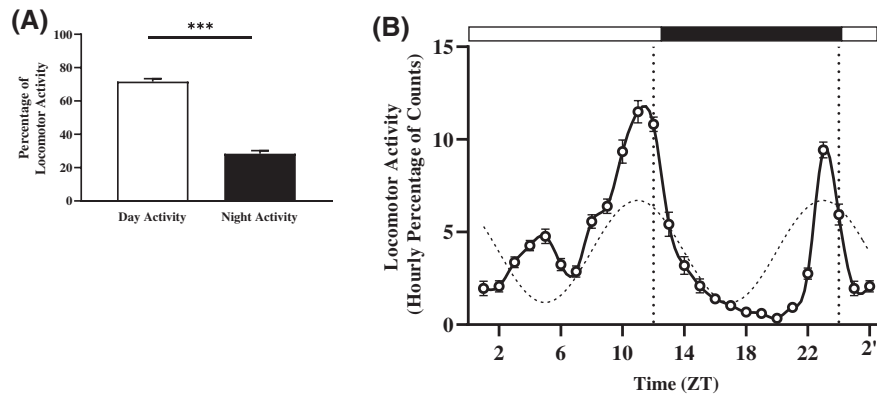
FIGURE 6 *Arvicanthis* plasma corticosterone levels measured by HPLC, in LD (A, open circles) and DD (B, filled circles). Points are connected by a smoothing line. ANOVA I analysis indicate a significant effect of time in LD ($p < .05$) and DD ($p < .01$). Dashed line represents the bimodal Cosinor fit in LD (A) and DD (B). Experimental groups were all $n = 6$, except for ZT6 ($n = 5$). Data are presented as mean ± SEM. Time is expressed as *Zeitgeber* time (ZT) or circadian time (CT). White and black horizontal bars represent light and dark phases, respectively

FIGURE 7 In panel A, percentage distribution of *Arvicanthis* locomotor activity between light (day activity, white bar) and dark (night activity, black bar) phases. Bars represent mean + SEM ($n = 17$, recording days = 4). Significance is expressed by three asterisks (***$p < .001$). In panel B, locomotor activity profile of *Arvicanthis* maintained in 12 h:12 h light/dark condition, plotted as hourly percentage of counts. Points are connected by a smoothing line. Points represent mean + SEM ($n = 17$, recording days = 4). The effect of time is significant ($p < .001$). Hourly data (open circles) are fitted by a bimodal Cosinor regression (dashed line). Time is expressed as *Zeitgeber* time (ZT) or circadian time (CT). White and black horizontal bars represent light and dark phases, respectively

are at ZT11.2 and ZT23.2, both occurring right after the peaks in corticosterone (ZT10.5 and ZT22.5).

4 | DISCUSSION

In the present study, we investigated serotonin synthesis in the diurnal rodent *Arvicanthis* by looking at serotonin rate-limiting enzyme, *tph2*. *Tph2* mRNA levels display a rhythmic bimodal profile over 24 h under both LD and DD conditions, showing that *tph2* rhythm persists in constant condition and is therefore endogenously regulated. Under both LD and DD cycles, higher levels of expression occurred around the (projected) light transitions. Of note, the *tph2* profiles observed in DD differed from that in LD. This finding suggests that light has an effect on serotonin synthesis, since it modifies the pattern of *tph2* endogenous rhythm. Among the SCN outputs studied, a bimodal profile was observed in corticosterone plasma levels in both LD and DD conditions, as well as in locomotor activity, which reflected *tph2* patterns. On the other hand, melatonin plasma rhythms in LD and DD were always unimodal with a peak during the night.

4.1 | Technical and anatomical consideration of *tph2* expression in *Arvicanthis*

Two isoforms of the rate-limiting enzyme of serotonin biosynthesis, TPH1 and TPH2, have been described in mammals.[42] The TPH2 isoform is predominant in the neurons and that of TPH1 in the peripheral organs, including the pineal gland.[26] In this study, we investigated

tph2 expression levels in the diurnal *Arvicanthis* using radioactive antisense riboprobe designed upon the rat *tph2* sequence to perform in situ hybridization in the RN. As *A. ansorgei* genome sequence has not been published yet, the similarity of our *tph2* riboprobe was tested on the *A. niloticus* genome, a species belonging to the same genus (https://www.ncbi.nlm.nih.gov/genome/annotation_euk/Arvicanthis_niloticus/100/). The high percentage (93.94%) of identity with the *tph2* predicted mRNA sequence demonstrated that it is suitable to detect *Arvicanthis tph2*. Specificity of the probe was confirmed by the absence of labelling in areas outside the RN and inside the RN when using the sense riboprobe. In addition, as was observed in rats,[26] hamsters[28] and mice,[43] *tph2* hybridization signals in *Arvicanthis* superimpose 5HT labelling, as previously shown by Adidharma and collegues.[44] Riboprobe hybridization allowed us to identify the anatomical extension of the RN in *Arvicanthis*. The architectural organisation of the RN has been previously described in other mammals (e.g., rats,[27] mice,[43] hamsters[28]), in which rostral, medial, and caudal parts of the DRN are delineated. In *Arvicanthis*, we distinguished the dorsal from the median raphe nuclei, and we considered the medial part of the DRN. We identified as medial DRN the portion of the DRN where we could distinguish the lateral, dorsomedial, and ventromedial subdivisions. We quantified *tph2* expression in these subgroups separately. Indeed, as previously shown in other mammals, these subregions may be considered as independent nuclei in accordance with receptor expression, electrophysiological properties, molecular organization and different afferent and efferent projections.[45-50] Furthermore, the RN subregions may be differently involved in the pathophysiology of depression, based on their sensitivity to anxiety and stress signals.[45]

4.2 | Rhythmic expression of *tph2* mRNA in the raphe nuclei of *Arvicanthis*

In *Arvicanthis*, serotonin synthesis is characterized by a bimodal rhythm. Within a given light condition (LD or DD), *tph2* expression shows similar profiles in all the RN structures, with higher levels around the light transitions. Under DD condition, *tph2* bimodality is evidenced by a 12 h-Cosinor fit in the Lat DRN and the MRN. Interestingly, among the RN subregions, those two are the structures more directly involved in the regulation of circadian rhythms. The MRN directly projects to the SCN,[51,52] while the two Lat DRN project to the IGL,[51] which in turn sends projections to the SCN.[53] Under the LD cycle, the bimodal expression of *tph2* mRNA levels persists. However, the *tph2* patterns differ between the LD and DD conditions.

The origin of *tph2* bimodality remains unclear as well as the mechanisms leading to different *tph2* profiles in LD vs DD. One hypothesis is that peaks of *tph2* expression occur at the transitions between (subjective) day/night and (subjective) night/day in both LD and DD conditions, but that in DD the whole curve is advanced. As shown in rats,[31] in *Arvicanthis tph2* expression could be driven by corticosterone (bimodal) rhythm. Although the overall phase of corticosterone rhythm does not change in DD compared to LD, Cosinor fit shows peaks in DD at CT9.5 and CT21.5, that is, 1 h in advance compared to the respective peaks in LD at ZT10.5 and ZT22.5. It is possible that, if the whole DD profile is advanced, it is partly due to corticosterone signals. Furthermore, locomotor activity may affect *tph2* levels.[31] In this study, locomotor activity data in DD are not available, but it cannot be excluded that locomotor activity peaks in DD are phase advanced as well. In an unpublished study, the period of locomotor activity in DD in *A. ansorgei* is shorter than 24 h. Therefore, it is possible that locomotor activity peaks are phase advanced after 2 days in DD. Finally, other light-dependent mechanisms may have an impact on *tph2* expression. Light influences the 5HT system not only through the circadian system (e.g. via corticosterone rhythm), but also via other pathways.[31,44,54] While in many rodent species, the DRN receives light information through direct projections from the retina,[55-57] a similar direct projection has not been observed in *Arvicanthis*.[58] Thus, in *Arvicanthis* light information may be conveyed to the 5HT system through other structures of the arousal system. For instance, orexin neurons, which are activated by light in *A. niloticus* but not in mice,[44,58,59,60] may mediate differential effects on the DRN activity between LD and DD, leading to changes in 24 h profiles of *tph2* mRNA levels. This strong difference between the LD and DD *tph2* profiles in *Arvicanthis* is not observed in nocturnal rats, in which LD and DD *tph2* profiles are similar.[26] These data suggest that light may have a stronger impact on serotonin synthesis in diurnal than in nocturnal rodents, and underscore the importance of using diurnal models for many research questions involving arousal structures like the serotonergic system.

4.3 | Bimodal rhythmic profiles of plasma corticosterone and locomotor activity in *Arvicanthis*

Plasma levels of corticosterone in *Arvicanthis* display a rhythmic bimodal profile in LD condition, with two peaks at the light transitions, in agreement with Verhagen et al.[61] Higher corticosterone levels were found at the end of the light and of the dark phases. Furthermore, a similar bimodal profile was detected in DD condition, highlighting that corticosterone bimodal rhythm is endogenous. Indeed, many studies have shown that glucocorticoid rhythm is under the control of the SCN.[62-64] Glucocorticoids surge has an anticipatory effect on locomotor activity.[65,66] Coherently, in our study we observed that the two peaks of corticosterone plasma levels precede the two peaks of locomotor activity observed at the light/dark transitions in LD. *Arvicanthis* corticosterone profile strongly differs from what has been observed in many species, where only one peak is measured.[67-70]

4.4 | Daily and circadian melatonin plasma levels in *Arvicanthis*

Melatonin is one of the principal outputs of the SCN and affects many structures in the brain and in the periphery.[71,72] In this study, we investigated melatonin plasma profile in *Arvicanthis*: we measured low melatonin level during the biological day and a peak at the end of the night, similarly to what has been shown in many nocturnal species and in humans.[73-79] Our data are coherent with the melatonin profile previously described in the *Arvicanthis* pineal gland in LD condition.[80] In addition, we showed a similar rhythm in DD condition, confirming that the melatonin rhythm is endogenous. Our findings agree with previous studies and with the sleep promoting effect of melatonin in diurnal but not in nocturnal species.[81-83]

4.5 | 5HT and 5HIAA levels in SCN in *Arvicanthis*

To gain more insights about serotonin synthesis in relation to *Arvicanthis* behavior, we evaluated the 5HT and 5HIAA SCN content at two time points of the biological

day and at the middle of the biological night, in LD and DD conditions. In our study, under LD condition, the effect of time was not significant. However, in DD we observed higher 5HT levels at the beginning of the subjective day compared to the middle of the subjective night. These data suggest that rhythm of 5HT in the SCN of *Arvicanthis* is endogenous. Finally, both LD and DD 5HT/5HIAA ratios, used as index of serotonin neuronal activity, were higher during the day than during the night, in relation to *Arvicanthis* activity state,[84] in accordance with Cuesta and colleagues.[40] A similar correlation with arousal has been shown in nocturnal rodents, where 5HT and 5HIAA content and release in the SCN is rhythmic and presents a peak at the beginning of the night (onset of activity).[29,85,86] Serotonin and 5HIAA rhythms are therefore in antiphase between nocturnal and diurnal rodents.

In DD condition, mean levels of 5HT, 5HIAA and 5HT/5HIAA ratio are lower than in LD condition. These findings are in accordance with a previous publication in Drosophila, showing that constant darkness decreases serotonin levels in the brain.[87] Furthermore, it corroborates the strong effect that light may have on serotonin, as previously shown on *tph2* levels.

In the nocturnal rat, a temporal sequential relationship was demonstrated between the rhythmic patterns of *tph2* mRNA in raphe cell bodies, the TPH2 protein and the 5HT release within the SCN.[26,27,29] Although 5HT/5HIAA ratio in the SCN is higher during the *Arvicanthis* active phase (Ref. [40], present study), the 5HT pattern of release in this species is still not known. Further investigation is necessary to assess whether the bimodal rhythm in serotonin synthesis is associated to a bimodal 5HT release in the SCN in *Arvicanthis*, and to elucidate the mechanisms leading from a bimodal 5HT synthesis to a unimodal rhythm in 5HT and 5HIAA content in the SCN.[40]

5 | CONCLUSION AND PERSPECTIVES

In this study, we characterized for the first time the *tph2* anatomical extension of the dorsal and median raphe nuclei of the diurnal *Arvicanthis*. We observed a bimodal rhythmic expression of *tph2* mRNA levels, and we demonstrated that the nature of this rhythm is endogenous. We correlated this bimodal *tph2* profile to the crepuscular locomotor activity rhythm of our animals, and to the bimodal corticosterone plasma levels. However, further experiments should be performed to confirm modulatory effects of locomotor activity and corticosterone on *tph2*

rhythm in *Arvicanthis*. Finally, 5HT/5HIAA ratio within the SCN of *Arvicanthis* is higher during the day (active phase) compared to the night (rest period).

Questions arise about the origin of bimodality in *Arvicanthis* and whether it directly depends on the SCN. According to the SCN outputs that we measured, the SCN rhythmic activity may be either bimodal (bimodal corticosterone rhythm) or unimodal (unimodal melatonin rhythm). This question could be potentially answered by electrical recording of the SCN in vitro.

Our data show that the circadian variations of the serotonergic system and the effect of light on its rhythms differ between nocturnal and diurnal rodents. These observations suggest that the serotonergic system may participate to the distinct temporal organization underlying nocturnality and diurnality. These findings in a diurnal mammal may be helpful for studies on human mood disorders, such as depression in which alteration of numerous biological rhythms including serotonin neurotransmission and sleep/wake cycles have been described.

DISCLOSURES
The authors declared no potential conflict of interest with respect to the research, authorship, and/or publication of this article.

AUTHOR CONTRIBUTIONS
Rosanna Caputo was involved in study design, data collection and interpretation, statistical analyses, and writing of the manuscript; Vincent-Joseph Poirel was involved in study design; Etienne Challet contributed to study conception and data interpretation; Johanna H. Meijer was involved in data interpretation; Sylvie Raison was involved in conception, design and coordination of the study, data interpretation and writing of the manuscript. All authors critically reviewed the manuscript and have approved the publication of this final version of the manuscript.

DATA AVAILABILITY STATEMENT

All raw data (autoradiographic films, actograms, HPLC and RIA assay data) that support the findings of this study are available on request from the corresponding author.

ORCID

Etienne Challet https://orcid.org/0000-0001-9416-9496

Sylvie Raison https://orcid.org/0000-0003-0977-5315

REFERENCES

1. Pittendrigh CS. Circadian rhythms and the circadian organization of living systems. *Cold Spring Harb Symp Quant Biol*. 1960;25:159-184.
2. Ralph MR, Foster RG, Davis FC, et al. Transplanted suprachiasmatic nucleus determines circadian period. *Science*. 1990;247(4945):975-978.
3. LeGates TA, Fernandez DC, Hattar S. Light as a central modulator of circadian rhythms, sleep and affect. *Nat Rev Neurosci*. 2014;15(7):443-454.
4. Manoogian ENC, Panda S. Circadian rhythms, time-restricted feeding, and healthy aging. *Ageing Res Rev*. 2017;39:59-67.
5. Rosenthal NE, Sack DA, Gillin JC, et al. Seasonal affective disorder. A description of the syndrome and preliminary findings with light therapy. *Arch Gen Psychiatry*. 1984;41(1):72-80.
6. Rastad C, Wetterberg L, Martin C. Patients' experience of winter depression and light room treatment. *Psychiatry J*. 2017;2017:6867957.
7. Bedrosian TA, Weil ZM, Nelson RJ. Chronic dim light at night provokes reversible depression-like phenotype: possible role for TNF. *Mol Psychiatry*. 2013;18(8):930-936.
8. Brown MJ, Jacobs DE. Residential light and risk for depression and falls: results from the LARES study of eight European cities. *Public Health Rep*. 2011;126(1_suppl):131-140.
9. Germain A, Kupfer DJ. Circadian rhythm disturbances in depression. *Hum Psychopharmacol*. 2008;23(7):571-585.
10. Daut RA, Fonken LK. Circadian regulation of depression: a role for serotonin. *Front Neuroendocrinol*. 2019;54:100746.
11. Mulinari S. Monoamine theories of depression: historical impact on biomedical research. *J Hist Neurosci*. 2012;21(4):366-392.
12. Perez-Caballero L, Torres-Sanchez S, Bravo L, et al. Fluoxetine: a case history of its discovery and preclinical development. *Expert Opin Drug Discov*. 2014;9(5):567-578.
13. Wong DT, Bymaster FP, Engleman EA. Prozac (fluoxetine, Lilly 110140), the first selective serotonin uptake inhibitor and an antidepressant drug: twenty years since its first publication. *Life Sci*. 1995;57(5):411-441.
14. Parker NG, Brown CS. Citalopram in the treatment of depression. *Ann Pharmacother*. 2000;34(6):761-771.
15. Lucki I. The spectrum of behaviors influenced by serotonin. *Biol Psychiatry*. 1998;44(3):151-162.
16. Young SN, Leyton M. The role of serotonin in human mood and social interaction. Insight from altered tryptophan levels. *Pharmacol Biochem Behav*. 2002;71(4):857-865.
17. Jordan LM, Liu J, Hedlund PB, et al. Descending command systems for the initiation of locomotion in mammals. *Brain Res Rev*. 2008;57(1):183-191.
18. Schmidt BJ, Jordan LM. The role of serotonin in reflex modulation and locomotor rhythm production in the mammalian spinal cord. *Brain Res Bull*. 2000;53(5):689-710.
19. Yannielli P, Harrington ME. Let there be "more" light: enhancement of light actions on the circadian system through non-photic pathways. *Prog Neurogibol*. 2004;74(1):59-76.
20. Bobrzynska KJ, Godfrey MH, Mrosovsky N. Serotonergic stimulation and nonphotic phase-shifting in hamsters. *Physiol Behav*. 1996;59(2):221-230.
21. Cutrera RA, Saboureau M, Pévet P. Phase-shifting effect of 8-OH-DPAT, a 5-HT1A/5-HT7 receptor agonist, on locomotor activity in golden hamster in constant darkness. *Neurosci Lett*. 1996;210(1):1-4.
22. Tominaga K, Shibata S, Ueki S, et al. Effects of 5-HT1A receptor agonists on the circadian rhythm of wheel-running activity in hamsters. *Eur J Pharmacol*. 1992;214(1):79-84.
23. Challet E. Minireview: entrainment of the suprachiasmatic clockwork in diurnal and nocturnal mammals. *Endocrinology*. 2007;148(12):5648-5655.
24. Cagampang FR, Inouye ST. Diurnal and circadian changes of serotonin in the suprachiasmatic nuclei: regulation by light and an endogenous pacemaker. *Brain Res*. 1994;639(1):175-179.
25. Dudley TE, DiNardo LA, Glass JD. Endogenous regulation of serotonin release in the hamster suprachiasmatic nucleus. *J Neurosci*. 1998;18(13):5045-5052.
26. Malek ZS, Dardente H, Pevet P, et al. Tissue-specific expression of tryptophan hydroxylase mRNAs in the rat midbrain: anatomical evidence and daily profiles. *Eur J Neurosci*. 2005;22(4):895-901.
27. Malek ZS, Pévet P, Raison S. Circadian change in tryptophan hydroxylase protein levels within the rat intergeniculate leaflets and raphe nuclei. *Neuroscience*. 2004;125(3):749-758.
28. Nexon L, Poirel V-J, Clesse D, et al. Complex regional influence of photoperiod on the nycthemeral functioning of the dorsal and median raphé serotoninergic system in the Syrian hamster. *Eur J Neurosci*. 2009;30(9):1790-1801.
29. Barassin S, Raison S, Saboureau M, et al. Circadian tryptophan hydroxylase levels and serotonin release in the suprachiasmatic nucleus of the rat. *Eur J Neurosci*. 2002;15(5):833-840.
30. Nexon L, Sage D, Pévet P, et al. Glucocorticoid-mediated nycthemeral and photoperiodic regulation of tph2 expression. *Eur J Neurosci*. 2011;33(7):1308-1317.
31. Malek ZS, Sage D, Pévet P, et al. Daily rhythm of tryptophan hydroxylase-2 messenger ribonucleic acid within raphe neurons is induced by corticoid daily surge and modulated by enhanced locomotor activity. *Endocrinology*. 2007;148(11):5165-5172.
32. Jacobs BL, Wilkinson LO, Fornal CA. The role of brain serotonin. A neurophysiologic perspective. *Neuropsychopharmacology*. 1990;3(5-6):473-479.
33. Refinetti R. The diversity of temporal niches in mammals. *Biol Rhythm Res*. 2008;39(3):173-192.
34. Cuesta M, Clesse D, Pévet P, et al. From daily behavior to hormonal and neurotransmitters rhythms: comparison between diurnal and nocturnal rat species. *Horm Behav*. 2009;55(2):338-347.
35. Caldelas I, Poirel V-J, Sicard B, et al. Circadian profile and photic regulation of clock genes in the suprachiasmatic nucleus

of a diurnal mammal *Arvicanthis ansorgei*. *Neuroscience*. 2003;116(2):583-591.

36. Dardente H, Menet JS, Challet E, et al. Daily and circadian expression of neuropeptides in the suprachiasmatic nuclei of nocturnal and diurnal rodents. *Brain Res Mol Brain Res*. 2004;124(2):143-151.

37. Sato T, Kawamura H. Circadian rhythms in multiple unit activity inside and outside the suprachiasmatic nucleus in the diurnal chipmunk (*Eutamias sibiricus*). *Neurosci Res*. 1984;1(1):45-52.

38. Challet E, Turek FW, Laute M-A, et al. Sleep deprivation decreases phase-shift responses of circadian rhythms to light in the mouse: role of serotonergic and metabolic signals. *Brain Res*. 2001;909(1-2):81-91.

39. Weber ET, Gannon RL, Rea MA. Local administration of serotonin agonists blocks light-induced phase advances of the circadian activity rhythm in the hamster. *J Biol Rhythms*. 1998;13(3):209-218.

40. Cuesta M, Mendoza J, Clesse D, et al. Serotonergic activation potentiates light resetting of the main circadian clock and alters clock gene expression in a diurnal rodent. *Exp Neurol*. 2008;210(2):501-513.

41. Paxinos G, Watson C. *The Rat Brain in Stereotaxic Coordinates*, 2nd ed. Sydney: Academic Press; 1986.

42. Sakowski SA, Geddes TJ, Thomas DM, et al. Differential tissue distribution of tryptophan hydroxylase isoforms 1 and 2 as revealed with monospecific antibodies. *Brain Res*. 2006;1085(1):11-18.

43. Fu W, Le Maître E, Fabre V, et al. Chemical neuroanatomy of the dorsal raphe nucleus and adjacent structures of the mouse brain. *J Comp Neurol*. 2010;518(17):3464-3494.

44. Adidharma W, Deats SP, Ikeno T, Lipton JW, Lonstein JS, Yan L. Orexinergic modulation of serotonin neurons in the dorsal raphe of a diurnal rodent, *Arvicanthis niloticus*. *Horm Behav*. 2019;116:104584.

45. Lowry CA, Hale MW, Evans AK, et al. Serotonergic systems, anxiety, and affective disorder: focus on the dorsomedial part of the dorsal raphe nucleus. *Ann N Y Acad Sci*. 2008;1148:86-94.

46. Huang KW, Ochandarena NE, Philson AC, et al. Molecular and anatomical organization of the dorsal raphe nucleus. *Elife*. 2019;8:e46464.

47. Clark MS, McDevitt RA, Neumaier JF. Quantitative mapping of tryptophan hydroxylase-2, 5-HT1A, 5-HT1B, and serotonin transporter expression across the anteroposterior axis of the rat dorsal and median raphe nuclei. *J Comp Neurol*. 2006;498(5):611-623.

48. Hensler JG, Ferry RC, Kovachich GB, et al. Quantitative autoradiography of the serotonin transporter to assess the distribution of serotonergic projections from the dorsal raphe nucleus. *Synapse*. 1994;17(1):1-15.

49. Jacobs BL, Azmitia EC. Structure and function of the brain serotonin system. *Physiol Rev*. 1992;72(1):165-229.

50. Kazakov VN, Kravtsov PYA, Krakhotkina ED, et al. Sources of cortical, hypothalamic and spinal serotonergic projections: topical organization within the nucleus raphe dorsalis. *Neuroscience*. 1993;56(1):157-164.

51. Meyer-Bernstein EL, Morin LP. Differential serotonergic innervation of the suprachiasmatic nucleus and the intergeniculate leaflet and its role in circadian rhythm modulation. *J Neurosci*. 1996;16(6):2097-2111.

52. Moga MM, Moore RY. Organization of neural inputs to the suprachiasmatic nucleus in the rat. *J Comp Neurol*. 1997;389(3):508-534.

53. Card JP, Moore RY. Organization of lateral geniculate-hypothalamic connections in the rat. *J Comp Neurol*. 1989;284(1):135-147.

54. Leach G, Adidharma W, Yan L. Depression-like responses induced by daytime light deficiency in the diurnal grass rat (*Arvicanthis niloticus*). *PLoS One*. 2013;8(2):e57115.

55. Shen H, Semba K. A direct retinal projection to the dorsal raphe nucleus in the rat. *Brain Res*. 1994;635(1-2):159-168.

56. Kawano H, Decker K, Reuss S. Is there a direct retina-raphe-suprachiasmatic nucleus pathway in the rat? *Neurosci Lett*. 1996;212(2):143-146.

57. Fite KV, Janusonis S. Retinal projection to the dorsal raphe nucleus in the Chilean degus (*Octodon degus*). *Brain Res*. 2001;895(1-2):139-145.

58. Adidharma W, Leach G, Yan L. Orexinergic signaling mediates light-induced neuronal activation in the dorsal raphe nucleus. *Neuroscience*. 2012;220:201-207.

59. Deats SP, Adidharma W, Lonstein JS, et al. Attenuated orexinergic signaling underlies depression-like responses induced by daytime light deficiency. *Neuroscience*. 2014;272:252-260.

60. Mendoza J, Clesse D, Pévet P, et al. Food-reward signalling in the suprachiasmatic clock. *J Neurochem*. 2010;112(6):1489-1499.

61. Verhagen LAW, Pévet P, Saboureau M, et al. Temporal organization of the 24-h corticosterone rhythm in the diurnal murid rodent *Arvicanthis ansorgei* Thomas 1910. *Brain Res*. 2004;995(2):197-204.

62. Abe K, Kroning J, Greer MA, et al. Effects of destruction of the suprachiasmatic nuclei on the circadian rhythms in plasma corticosterone, body temperature, feeding and plasma thyrotropin. *Neuroendocrinology*. 1979;29(2):119-131.

63. Moore RY, Eichler VB. Loss of a circadian adrenal corticosterone rhythm following suprachiasmatic lesions in the rat. *Brain Res*. 1972;42(1):201-206.

64. Buijs RM, Kalsbeek A, van der Woude TP, et al. Suprachiasmatic nucleus lesion increases corticosterone secretion. *Am J Physiol*. 1993;264(6 Pt 2):R1186-R1192.

65. Kalsbeek A, van der Vliet J, Buijs RM. Decrease of endogenous vasopressin release necessary for expression of the circadian rise in plasma corticosterone: a reverse microdialysis study. *J Neuroendocrinol*. 1996;8(4):299-307.

66. Sage D, Ganem J, Guillaumond F, et al. Influence of the corticosterone rhythm on photic entrainment of locomotor activity in rats. *J Biol Rhythms*. 2004;19(2):144-156.

67. Allen-Rowlands CF, Allen JP, Greer MA, et al. Circadian rhythmicity of ACTH and corticosterone in the rat. *J Endocrinol Invest*. 1980;3(4):371-377.

68. Dalm S, Enthoven L, Meijer OC, et al. Age-related changes in hypothalamic-pituitary-adrenal axis activity of male C57BL/6J mice. *Neuroendocrinology*. 2005;81(6):372-380.

69. Albers HE, Yogev L, Todd RB, et al. Adrenal corticoids in hamsters: role in circadian timing. *Am J Physiol*. 1985;248(4 Pt 2):R434-R438.

70. Weitzman ED, Fukushima D, Nogeire C, et al. Twenty-four hour pattern of the episodic secretion of cortisol in normal subjects. *J Clin Endocrinol Metab*. 1971;33(1):14-22.

71. Meijer JH, Rietveld WJ. Neurophysiology of the suprachiasmatic circadian pacemaker in rodents. *Physiol Rev.* 1989;69(3):671-707.

72. Pévet P. Melatonin. *Dialogues Clin Neurosci.* 2002;4(1):57-72.

73. Gündüz B. Daily rhythm in serum melatonin and leptin levels in the Syrian hamster (*Mesocricetus auratus*). *Comp Biochem Physiol A Mol Integr Physiol.* 2002;132(2):393-401.

74. Kennaway DJ, Voultsios A, Varcoe TJ, et al. Melatonin in mice: rhythms, response to light, adrenergic stimulation, and metabolism. *Am J Physiol Regul Integr Comp Physiol.* 2002;282(2):R358-R365.

75. Lewy AJ, Tetsuo M, Markey SP, et al. Pinealectomy abolishes plasma melatonin in the rat. *J Clin Endocrinol Metab.* 1980;50(1):204-205.

76. Niklowitz P, Lerchl A, Nieschlag E. Photoperiodic responses in Djungarian hamsters (*Phodopus sungorus*): importance of light history for pineal and serum melatonin profiles. *Biol Reprod.* 1994;51(4):714-724.

77. Panke ES, Rollag MD, Reiter RJ. Pineal melatonin concentrations in the Syrian hamster. *Endocrinology.* 1979;104(1):194-197.

78. Zeitzer JM, Duffy JF, Lockley SW, et al. Plasma melatonin rhythms in young and older humans during sleep, sleep deprivation, and wake. *Sleep.* 2007;30(11):1437-1443.

79. Zhdanova IV, Wurtman RJ, Balcioglu A, et al. Endogenous melatonin levels and the fate of exogenous melatonin: age effects. *J Gerontol A Biol Sci Med Sci.* 1998;53(4):B293-B298.

80. Garidou ML, Gauer F, Vivien-Roels B, Sicard B, Pévet P, Simonneaux V. Pineal arylalkylamine N-acetyltransferase gene expression is highly stimulated at night in the diurnal rodent, *Arvicanthis ansorgei. Eur J Neurosci.* 2002;15(10):1632-1640.

81. Gandhi A, Mosser EA, Oikonomou G, et al. Melatonin is required for the circadian regulation of sleep. *Neuron.* 2015;85(6):1193-1199.

82. Fisher SP, Foster RG, Peirson SN. The circadian control of sleep. *Handb Exp Pharmacol.* 2013;217:157-183.

83. Zhdanova IV. Melatonin as a hypnotic: pro. *Sleep Med Rev.* 2005;9(1):51-65.

84. Flaive A, Fougère M, van der Zouwen CI, Ryczko D. Serotonergic modulation of locomotor activity from basal vertebrates to mammals. *Front Neural Circuits.* 2020;14:590299.

85. Garabette ML, Martin KF, Redfern PH. Circadian variation in the activity of the 5-HT(1B) autoreceptor in the region of the suprachiasmatic nucleus, measured by microdialysis in the conscious freely-moving rat. *Br J Pharmacol.* 2000;131(8):1569-1576.

86. Knoch ME, Gobes SMH, Pavlovska I, et al. Short-term exposure to constant light promotes strong circadian phase-resetting responses to nonphotic stimuli in Syrian hamsters. *Eur J Neurosci.* 2004;19(10):2779-2790.

87. Yuan Q, Lin F, Zheng X, et al. Serotonin modulates circadian entrainment in Drosophila. *Neuron.* 2005;47(1):115-127.

SUPPORTING INFORMATION

Additional supporting information may be found in the online version of the article at the publisher's website.